

ARRANGE AND AVERAGE ALGORITHM FOR MICROPHYSICAL RETRIEVALS WITH A “ $3\beta+3\alpha$ ” LIDAR CONFIGURATION

Eduard Chemyakin^{1*}, Detlef Müller^{1,2}, Sharon Burton³, Chris Hostetler³, Richard Ferrare³

¹Science Systems and Applications, Inc., NASA Langley Research Center,
 Mail Stop 475, Hampton, Virginia 23681-2199, USA, *Email: eduard.v.chemyakin@nasa.gov

²University of Hertfordshire, College Lane, Hatfield, AL10 9AB Hertfordshire, UK

³NASA Langley Research Center, Mail Stop 401 A, Hampton, Virginia 23681-2199, USA

ABSTRACT

We present the results of a comparison study in which a simple, automated, and unsupervised algorithm, which we call the arrange and average algorithm, was used to infer microphysical parameters (complex refractive index (CRI), effective radius, total number, surface area, and volume concentrations) of atmospheric aerosol particles. The algorithm normally uses backscatter coefficients (β) at 355, 532, and 1064 nm and extinction coefficients (α) at 355 and 532 nm as input information. We compared the performance of the algorithm for the existing “ $3\beta+2\alpha$ ” and potential “ $3\beta+3\alpha$ ” configurations of a multiwavelength aerosol Raman lidar or high-spectral-resolution lidar (HSRL). The “ $3\beta+3\alpha$ ” configuration uses an extra extinction coefficient at 1064 nm. Testing of the algorithm is based on synthetic optical data that are computed from prescribed CRIs and monomodal logarithmically normal particle size distributions that represent spherical, primarily fine mode aerosols. We investigated the degree to which the microphysical results retrieved by this algorithm benefits from the increased number of input extinction coefficients.

1. INTRODUCTION

Aerosol particles affect the radiative energy balance in the atmosphere and thus influence Earth's climate [1]. Different types of aerosols, e.g., sea salt, desert dust, smoke from biomass burning, and emissions from the burning of fossil fuel, influence regional and global climate through the direct and indirect radiative effect, which may result in net cooling or net warming of the air, changes of the large-scale atmospheric circulation, cloud lifetime and occurrence, and intensity of precipitation [1]. In this context, light

detection and ranging (lidar) instruments will play an important role as only these instruments provide information of aerosol properties on a comparably high vertical resolution. There are several fundamental approaches that allow one to retrieve microphysical parameters of aerosols from combinations of backscatter and extinction coefficients. The main techniques are Tikhonov's inversion with regularization [2–6], principal components analysis [7; 8], linear estimation [9], and recently we presented the arrange and average algorithm [10]. In our paper we considered four existing lidar configurations [10]. In this study we investigate if a “ $3\beta+3\alpha$ ” configuration has potential advantage over a “ $3\beta+2\alpha$ ” configuration. We have not seen yet any publication stating that the extinction coefficient at 1064 nm was successfully measured using Raman or HSRL technology but the “ $3\beta+3\alpha$ ” configuration is still possible via combination of lidar and column measurements of the atmospheric optical depth at 1064 nm. We investigated if this extra extinction coefficient could have a significant effect on the retrieval accuracy of microphysical properties.

2. METHODOLOGY

The general structure of the arrange and average algorithm is shown in study [10]. Few minor changes were done to adapt the algorithm for the needs of the “ $3\beta+3\alpha$ ” configuration. We increased the number of employed input optical data ratios from 11 for the “ $3\beta+2\alpha$ ” to 15 for the “ $3\beta+3\alpha$ ” lidar configuration [10]. The updated list contains six normalized input optical data

$$\beta_{355}^* = \frac{\beta_{355}}{\beta_3}, \quad \beta_{532}^* = \frac{\beta_{532}}{\beta_3}, \quad \beta_{1064}^* = \frac{\beta_{1064}}{\beta_3},$$

where $\beta_3 = \sqrt{\beta_{355}^2 + \beta_{532}^2 + \beta_{1064}^2}$, and

$$\alpha_{355}^* = \frac{\alpha_{355}}{\alpha_3}, \quad \alpha_{532}^* = \frac{\alpha_{532}}{\alpha_3}, \quad \alpha_{1064}^* = \frac{\alpha_{1064}}{\alpha_3},$$

where $\alpha_3 = \sqrt{\alpha_{355}^2 + \alpha_{532}^2 + \alpha_{1064}^2}$, and also we use nine extinction-to-backscatter ratios:

$$\begin{aligned} c_{355}^{355} &= \frac{\alpha_{355}}{\beta_{355}}, & c_{532}^{355} &= \frac{\alpha_{355}}{\beta_{532}}, & c_{1064}^{355} &= \frac{\alpha_{355}}{\beta_{1064}}, \\ c_{355}^{532} &= \frac{\alpha_{532}}{\beta_{355}}, & c_{532}^{532} &= \frac{\alpha_{532}}{\beta_{532}}, & c_{1064}^{532} &= \frac{\alpha_{532}}{\beta_{1064}}, \\ c_{355}^{1064} &= \frac{\alpha_{1064}}{\beta_{355}}, & c_{532}^{1064} &= \frac{\alpha_{1064}}{\beta_{532}}, & c_{1064}^{1064} &= \frac{\alpha_{1064}}{\beta_{1064}}. \end{aligned}$$

Thus, we kept the concept of using ratios of backscatter and extinction coefficients which allows to compare the pre-calculated and arbitrary optical data sets [10]. As the result of calibration simulations [10], the value of the reduction coefficient was increased from $w_{3\beta+2\alpha}=0.375$ to $w_{3\beta+3\alpha}=0.476$. The core of the arrange and average algorithm, i. e., the look-up table was used without any changes [10].

3. RESULTS

We performed numerical simulations using noise-free optical data. Figures 1–6 present the results. The figures display the statistical distribution of precision, which is achievable for the “ $3\beta+3\alpha$ ” and “ $3\beta+2\alpha$ ” lidar configurations. The left vertical axis of each plot shows the number of cases (the total number was 2880 optical data sets) that were tested [10]. The histogram displays the statistical distribution of errors of the retrieved microphysical parameters. The right vertical axis of each plot refers to the cumulative probability distribution. The cumulative probabilities are shown for the positive and for the negative retrieval errors. The left and right axes on the plots are scaled to each other. The maximum value of 61% shown on the right axis (“Cumulative probability, %”) corresponds to the value of 1750 shown on the left axis (“Number of cases”). Positive values of the horizontal axes mean that the retrieval results overestimated the true values. Negative values show that the retrieval results underestimated the true values. Figures 1 and 2 show the retrieval statistics for the real and imaginary parts of the CRI. The horizontal axis of Figure 1 is split in increments of 0.05. We chose the stepsize of 0.05 because our goal is to achieve a precision of 0.05 for the retrieved real part of the CRI. The horizontal axis of Figure 2 is incremented in steps of 0.005, which we target regarding the retrieval precision

of the imaginary part. Figures 3–6 show the statistics of the retrieved value of effective radius, total number, surface area, and volume concentrations. The stepsize in each case is 10%. In contrast to the CRI we show the results in terms of relative error. We consider 10% relative precision to be an ambitious goal for any algorithm that is used for the retrieval of these parameters. Table 1 summarizes the statistics of the parameters retrieved with the automated, unsupervised arrange and average algorithm for all 2880 optical data for both lidar configurations. The precision of the total number concentration estimation is worse than for any other size property. Considering all simulated cases, the effective radius has the smallest values of relative error (see the “100%” subcolumn) and has the same order of magnitude as the true effective radius in the majority of cases. The total surface area concentration has the smallest retrieval uncertainties with regard to the “68.2%” subcolumn (see the well-pronounced central peaks in Figure 5). The usage of an extra extinction coefficient by “ $3\beta+3\alpha$ ” configuration allows to reduce the maximal value of retrieval error for all size properties (see the “100%” subcolumn).

4. CONCLUSIONS

Using our novel arrange and average algorithm we estimated its performance for one extra lidar configuration. The “ $3\beta+3\alpha$ ” option was skipped in our key publication [10]. The comparison between the most advanced of existing “ $3\beta+2\alpha$ ” and potential “ $3\beta+3\alpha$ ” lidar configurations was done by using only noiseless input data. We obtained a quick-look impression about benefits of the increase of the number of extinction coefficients being used for the retrievals. The best overall performance of the arrange and average algorithm in this study was achieved with the “ $3\beta+3\alpha$ ” configuration, however the benefit of this extra extinction coefficient does not seem to be significant. The “ $3\beta+2\alpha$ ” results statistically are slightly worse. Thus, we confirmed a similar trend that was noticed earlier, i. e., the increase of number of used optical coefficients slowly improves the precision of microphysical products [10].

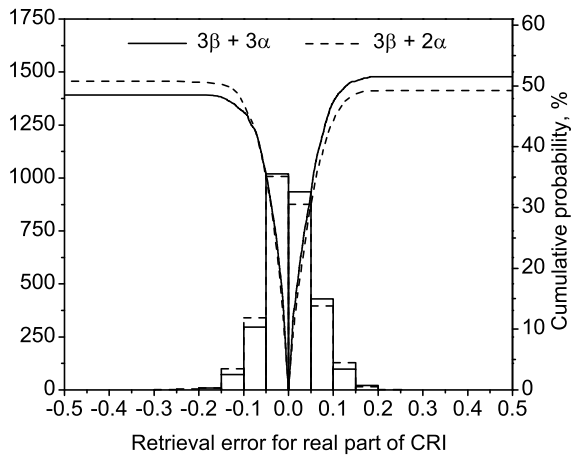


Figure 1: Retrieval of the real part of the CRI for the “ $3\beta+3\alpha$ ” lidar configuration (solid line) and the “ $3\beta+2\alpha$ ” configuration (dashed line). Negative values indicate overestimation in the retrievals whereas positive values mean underestimation.

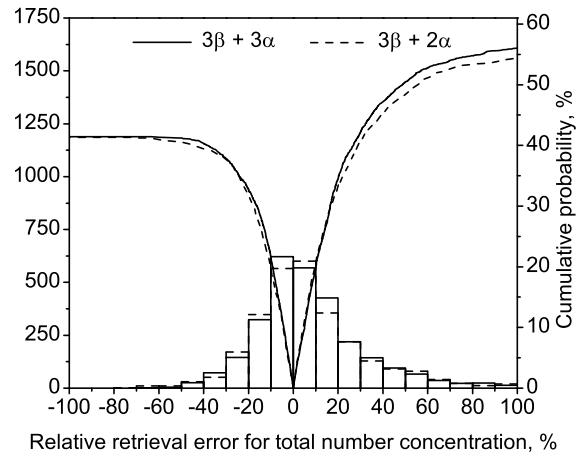


Figure 4: Retrieval of the total number concentration. The notation is the same as in Figure 1.

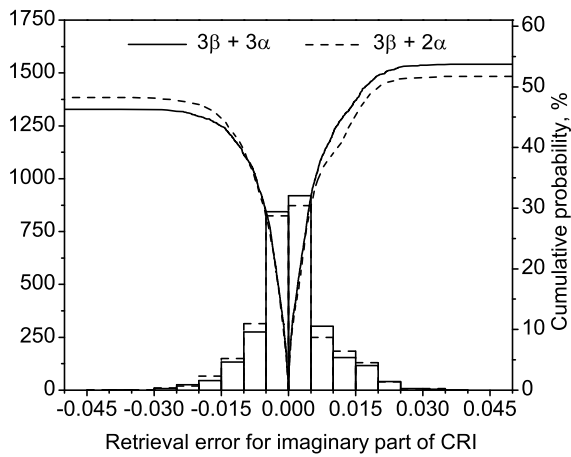


Figure 2: Retrieval of the imaginary part of the CRI. The notation is the same as in Figure 1.

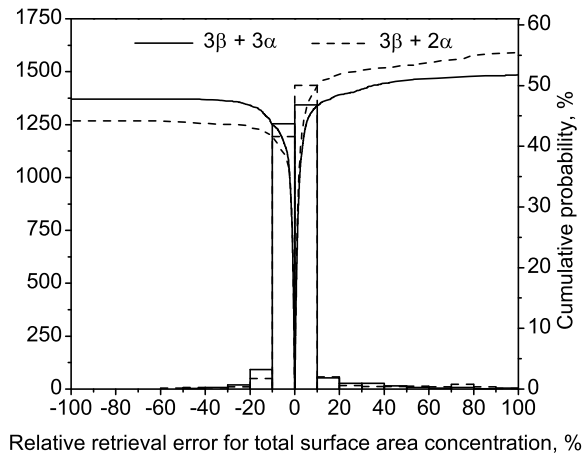


Figure 5: Retrieval of the total surface area concentration. The notation is the same as in Figure 1.

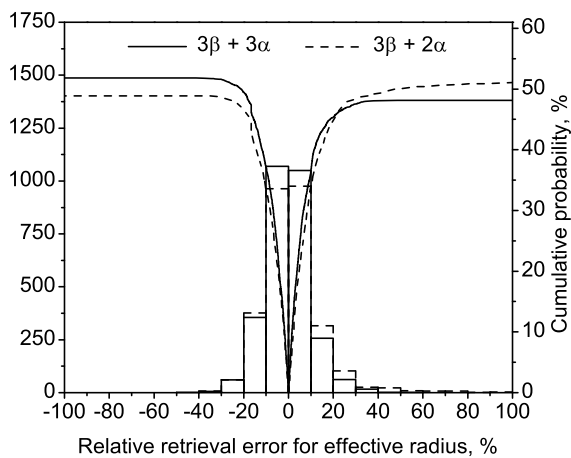


Figure 3: Retrieval of the effective radius. The notation is the same as in Figure 1.

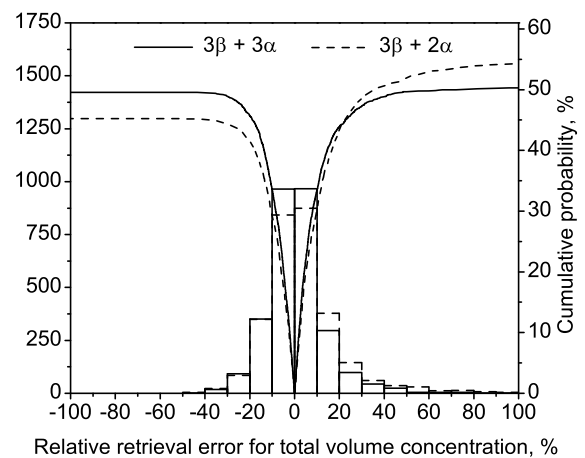


Figure 6: Retrieval of the total volume concentration. The notation is the same as in Figure 1.

Table 1: Retrieval Errors for the Microphysical Parameters^a

Lidar Configuration	68.2%	95.4%	100%
Retrieval error for real part of CRI			
" $3\beta+3\alpha$ "	0.051	0.114	0.184
" $3\beta+2\alpha$ "	0.054	0.116	0.256
Retrieval error for imaginary part of CRI			
" $3\beta+3\alpha$ "	0.0063	0.0182	0.0374
" $3\beta+2\alpha$ "	0.0067	0.0182	0.0313
Relative retrieval error for effective radius, %			
" $3\beta+3\alpha$ "	9	21	54
" $3\beta+2\alpha$ "	10	25	107
Relative retrieval error for total number concentration, %			
" $3\beta+3\alpha$ "	20	70	340
" $3\beta+2\alpha$ "	22	94	2218
Relative retrieval error for total surface area concentration, %			
" $3\beta+3\alpha$ "	2	21	186
" $3\beta+2\alpha$ "	2	21	253
Relative retrieval error for total volume concentration, %			
" $3\beta+3\alpha$ "	10	28	125
" $3\beta+2\alpha$ "	12	38	173

^aShown are the precisions being achieved for 68.2% (analog of one-standard deviation), 95.4% (analog of two-standard deviations), and 100% out of 2880 of optical data.

REFERENCES

1. Solomon, S., D. Qin, M. Manning, M. Marquis, K. Averyt, M. Tignor, H. Miller, Z. Chen, 2007: The Physical Science Basis. Contribution of Working Group I to the Fourth Assessment Report of the Intergovernmental Panel on Climate Change, *Cambridge University Press, Cambridge*.
2. Müller, D., U. Wandinger, A. Ansmann, 1999: Microphysical particle parameters from extinction and backscatter lidar data by inversion with regularization: theory, *Appl. Opt.*, **38**, 2346-2357.
3. Müller, D., U. Wandinger, A. Ansmann, 1999: Microphysical particle parameters from extinction and backscatter lidar data by inversion with regularization: simulation, *Appl. Opt.*, **38**, 2358-2368.
4. Veselovskii, I., A. Kolgotin, V. Griaznov, D. Müller, U. Wandinger, D. N. Whiteman, 2002: Inversion with regularization for the retrieval of

tropospheric aerosol parameters from multiwavelength lidar sounding, *Appl. Opt.*, **41**, 3685-3699.

5. Veselovskii, I., A. Kolgotin, V. Griaznov, D. Müller, K. Franke, D. N. Whiteman, 2004: Inversion of multiwavelength Raman lidar data for retrieval of bimodal aerosol size distribution, *Appl. Opt.*, **43**, 1180-1195.

6. Kolgotin, A., D. Müller, 2008: Theory of inversion with two-dimensional regularization: profiles of microphysical particle properties derived from multiwavelength lidar measurements, *Appl. Opt.*, **47**, 4472-4490.

7. Donovan, D. P., A. I. Carswell, 1997: Principle component analysis applied to multiwavelength lidar aerosol backscatter and extinction measurements, *Appl. Opt.*, **36**, 9406-9424.

8. De Graaf, M., A. Apituley, D. Donovan, 2013: Feasibility study of integral property retrieval for tropospheric aerosol from Raman lidar data using principal component analysis, *Appl. Opt.*, **52**, 2173-2186.

9. Veselovskii, I., O. Dubovik, A. Kolgotin, M. Korenskiy, D. N. Whiteman, K. Allakhverdiev, F. Huseyinoglu, 2012: Linear estimation of particle bulk parameters from multiwavelength lidar measurements, *Atmos. Meas. Tech.*, **5**, 1135-1145.

10. Chemyakin, E., D. Müller, S. Burton, A. Kolgotin, C. Hostetler, R. Ferrare, 2014: Arrange and average algorithm for the retrieval of aerosol parameters from multiwavelength high-spectral-resolution lidar / Raman lidar data, *Appl. Opt.*, **53**, 7252-7266.